

# Biocompatibility Testing of UV-Curable Polydimethylsiloxane for Human Umbilical Vein Endothelial Cell Culture on-a-Chip

Ana I. Gómez-Varela,<sup>\*</sup> Antonio Viña,<sup>°</sup> Carmen Bao-Varela, María Teresa Flores-Arias, Bastián Carnero, Mercedes González-Peteiro, José Ramón González-Juanatey, and Ezequiel Álvarez



Cite This: *ACS Omega* 2024, 9, 30281–30293



Read Online

ACCESS |

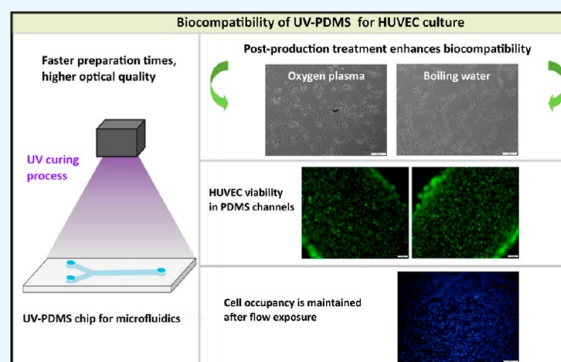
Metrics & More

Article Recommendations

Supporting Information

**ABSTRACT:** Polydimethylsiloxane (PDMS) is extensively used to fabricate biocompatible microfluidic systems due to its favorable properties for cell culture. Recently, ultraviolet-curable PDMS (UV-PDMS) has shown potential for enhancing manufacturing processes and final optical quality while retaining the benefits of traditional thermally cured PDMS. This study investigates the biocompatibility of UV-PDMS under static and flow conditions using human umbilical vein endothelial cells (HUVECs). UV-PDMS samples were treated with oxygen plasma and boiling deionized water to assess potential improvements in cell behavior compared with untreated samples. We evaluated HUVECs adhesion, growth, morphology, and viability in static cultures and microchannels fabricated with UV-PDMS to test their resistance to flow conditions. Our results confirmed the biocompatibility of UV-PDMS for HUVECs culture.

Moreover, plasma-oxygen-treated UV-PDMS substrates exhibited superior cell growth and adhesion compared to untreated UV-PDMS. This enhancement enabled HUVECs to maintain their morphology and viability under flow conditions in UV-PDMS microchannels. Additionally, UV-PDMS demonstrated improved optical quality and more efficient handling and processing, characterized by shorter curing times and simplified procedures utilizing UV light compared to traditional PDMS.



## 1. INTRODUCTION

Research on new biocompatible materials for the development of microfluidic chips is important because these materials play a crucial role in ensuring the safe and effective functioning of the chips. Microfluidic chips are used in a wide range of applications, including medical diagnosis and drug discovery, and they rely on the movement of small volumes of fluids through tiny channels.<sup>1</sup> If they are devoted to organ-on-a-chip, they may support cell culture inside, so they need to be biocompatible.<sup>2,3</sup> Biocompatible materials are those that are safe for use in contact with living tissue, and they are essential for ensuring that the microfluidic chips do not cause harm to the biological samples being studied. Additionally, biocompatible materials can also improve the performance and reliability of microfluidic chips, making them more effective and useful for a variety of applications.<sup>4</sup> Polydimethylsiloxane (PDMS) is the most widely used polymer for microfluidic applications involving cell seeding and culturing. It functions similarly to a resin: a compound that, under specific processes such as curing, can polymerize and adopt a solid structure. This method of fabrication, along with the resultant properties, supports its utility in microfluidic organ-on-a-chip systems due to several advantages: simple and cost-effective manufacturing techniques, precise reproducibility of shape, optical transparency, good thermal stability, impressive weather, and

chemical resistance, coupled with suitable attributes for biological applications such as high gas permeability, biocompatibility, and nontoxicity.<sup>5</sup>

There are several methods for curing PDMS, each with its own set of advantages. Thermally cured PDMS is most commonly used in microfluidic applications involving cell seeding and culturing. It is typically fabricated using a two-part liquid silicone elastomer kit that contains a base polymer and a curing agent. The base and curing agent are mixed together in a given ratio (depending on the specific kit), and then the mixture is poured into a mold or onto a substrate. The mixture is subsequently cured at an elevated temperature (usually around 70–100 °C) for several hours to cross-link the polymer chains and form a solid elastomer. Nevertheless, this type of curing chemistry presents certain drawbacks, including the environmental harm caused by heavy metal catalysts as well as requirements for high curing temperatures and elevated energy consumption.

**Received:** February 5, 2024

**Revised:** June 7, 2024

**Accepted:** June 12, 2024

**Published:** July 1, 2024



In order to be more environmentally friendly and energy-efficient, photocuring techniques, especially ultraviolet (UV) curing, are increasingly being used. UV curing has several benefits, such as low energy consumption, high efficiency, no need for solvents, and gentle reaction conditions (room temperature), being considered an eco-friendly technique.<sup>6,7</sup> UV-curable PDMS (UV-PDMS) is, therefore, cured using UV light and presents some advantages over thermally cured PDMS. First, the faster curing time as UV-cured PDMS typically cures in minutes compared to several hours for thermally cured PDMS. Thermal curing also typically requires higher temperatures to accomplish the process. Another advantage is that UV-curing can be precisely controlled in terms of intensity, duration, and spatial distribution, which can be advantageous for applications where precise patterning or shaping is required.<sup>8</sup> UV-cured PDMS typically experiences less shrinkage during curing, which can be beneficial for applications where dimensional stability is critical.<sup>9</sup> Furthermore, UV-curing of resins provides an opportunity to explore novel and enhanced photoinitiators. These low-molecular-weight compounds have the potential to optimize the curing process by refining reaction conditions and augmenting polymerization, ultimately enhancing the structural stability of silicone resins.<sup>10</sup>

An integral aspect of this progression involves the introduction of UV/thermal curing silicone polymers. A common challenge in UV curing is the occurrence of shadow areas, where curing levels cannot be assured, potentially compromising the final product performance. However, systems incorporating both photosensitive and thermosensitive groups can sequentially undergo both curing processes, mitigating this issue. This dual approach not only ensures deeper curing but also enhances the polymer performance. While this technology is still in its nascent stage and demands a higher cost compared to UV curing, its potential is substantial across various fields, including biomedicine. Such dual curing systems hold promise for expanding the applications of UV curing, facilitating the production of thick layers, colored coatings, and UV/thermal two-stage curing in three-dimensional (3D) printing.<sup>11</sup>

While PDMS is widely recognized as a standout polymer in microfluidics for biological applications such as cell culture, its inherent hydrophobic nature presents challenges for efficient cell attachment. Consequently, such materials often require postcuring treatments to fully exploit their beneficial properties in biological applications. Numerous studies have therefore been conducted to enhance cellular attachment on PDMS surfaces.<sup>12</sup> Cellular attachment can be influenced not only by the physiochemical properties of PDMS but also by the cell culture type,<sup>13</sup> so biocompatibility testing should be previously carried out for each particular application. Various techniques have been developed to increase cell adhesion on PDMS surfaces, including chemical modifications, physical treatments, and plasma-based methods. Oxygen plasma treatment (OPT)<sup>14,15</sup> and UV/ozone treatment are two commonly used methods to introduce oxygen-containing functional groups on the surface of PDMS, which promote cell adhesion.<sup>16–18</sup> The surface of the PDMS can also be modified with various chemicals or biomolecules to promote cell adhesion. For example, silanes such as 3-aminopropyltriethoxysilane or poly-L-lysine can be used to create amine groups on the surface, which can enhance cell adhesion.<sup>19</sup> Other molecules, such as fibronectin or laminin can also be

immobilized on the surface of PDMS to provide specific cell-binding sites.<sup>20</sup> In addition, physical treatments such as wet heating with boiling water, mechanical abrasion, micro/nanostructuring, and laser patterning can modify the surface of PDMS to enhance cell adhesion by increasing the surface area or providing specific surface patterns for cell attachment.<sup>21–23</sup> These approaches provide researchers with a range of options for optimizing PDMS surfaces to promote cell adhesion and improve their utility in various applications, such as microfluidic devices and cell culture platforms. It is worth noting that while enhancing cell adhesion can be beneficial for certain applications, it can also affect the mechanical and surface properties of PDMS. Therefore, it is important to carefully consider the specific requirements of the application when choosing a method to enhance PDMS cell adhesion.

In summary, our study aimed to achieve two primary objectives: first, to assess the biocompatibility of UV-cured PDMS compared to conventionally used thermally cured PDMS for human endothelial cell culture; and second, to investigate two postcuring methods intended for enhancing cell attachment and growth on UV-PDMS surfaces. One approach involved subjecting UV-PDMS samples to OPT, while the other method entailed immersing UV-PDMS in boiling water to introduce hydroxyl functional groups that promote cellular adhesion.<sup>23</sup>

## 2. MATERIALS AND METHODS

**2.1. Preparation of PDMS and UV-PDMS.** Two types of PDMS were used: thermally cured PDMS and UV-PDMS. In the first case, PDMS was prepared from commercial SYLGAR 184 elastomer (Dow Chemical Company, Midland, Michigan). It was supplied as a two-part liquid system (a prepolymer base and a cross-linking agent) that, when mixed, was curable at either room temperature or higher temperatures. The PDMS precursor synthesis was done by mixing the PDMS base and the cross-linking agent at a weight ratio of 10:1 and stirring uniformly in accordance with the supplier's recommendations. This mixture was then degassed into a vacuum chamber to remove air bubbles induced during mixing. A curing protocol with a temperature ramp was applied to avoid the formation of air bubbles, as follows: start temperature from room temperature to 60 °C with a 30 min ramp time and curing time of 12 h. Afterward, the sample was allowed to cool to room temperature.

UV-PDMS was prepared from KER-4690 A/B (Shin-Etsu Europe BV). It consists of two components, KER-4690-A and KER-4690-B, that the manufacturer recommends mixing in a 50:50 weight ratio. However, in our preliminary experiments, different ratios of the two components in the range 40–60% were studied to select the best mixing ratio for our purpose. The mixture was degassed under the same conditions as stated above and totally cured by irradiation to a 405 nm LED flood at 5.34 mW/cm<sup>2</sup> for 10 min in a chamber heated at 50 °C (FormCure, Formlabs Somerville, Massachusetts, USA). This specific combination of curing conditions for PDMS yielded homogeneous curing of the material with efficient processing time, although alternative combinations of temperature and UV exposure can also be utilized.

For the biocompatibility assays, both PDMS and UV-PDMS precursors were casted in a master glass Petri dish (40 mm in diameter) and subsequently cured using the thermal- or UV-curing treatments, as described above.

For the *in vitro* studies under flow conditions, chips with Y-shaped channels with a circular internal section of 2 mm of diameter were fabricated with UV-PDMS. To obtain chips with this geometry, semi blood vessel-like devices were manufactured and subsequently sealed as two-halves to obtain the final circular-internal section of Y-shaped channels. The master molds were designed using a CAD (computer-aided design) software and fabricated from Clear V4 commercial resin (Formlabs, Somerville, Massachusetts, USA) by low-force stereolithography using a 3D printer (Form 3B printer, Formlabs, Somerville, Massachusetts). Once the masters were ready, they were replicated by filling the structure with UV-PDMS to obtain the reverse structure. After degasification to remove the air bubbles in the mixture, the silicone master covered with UV-PDMS was cured using an UV lamp (405 nm), following the treatment, as indicated above. Subsequently, the UV-PDMS chip was demolded and bonded to another chip by the oxygen plasma technique with a Diener Zepto plasma cleaner (Diener Electronic GmbH, Jettingen, Germany). Next, the samples were subjected to a thermal treatment of 30 min at 90 °C to enhance the optical quality of the device for microscope inspection and to promote the sealing of the two parts of the chip.

**2.2. UV-PDMS Surface Modification Treatments.** After the UV-PDMS samples were cured, their surfaces were subjected to different treatments to improve their biocompatibility properties. Hence, we prepared the following sets of conditions: (1) UV-PDMS without a subsequent surface treatment (called T1); (2) UV-PDMS surface treated with boiling deionized water, by immersing the sample into a beaker with boiling deionized water for 1 h (T2); and (3) OPT, in which the samples were introduced into a plasma chamber for oxygen plasma activation at a pressure of 0.4 mbar (oxygen flow rate of 0.2 Nl/h) and 50 W for 60 s (T3). The samples prepared by these proceedings were used for cell biocompatibility experiments measuring cell adhesion to the surface, cell growth, and F-actin filament arrangement.

A second set of samples was prepared to evaluate possible differences in cell biocompatibility for different OPTs. Thus, UV-PDMS substrates were subjected to an OPT of different durations: 10, 20, 40, and 60 s. In all cases, OPT treatments were carried out with the above-mentioned oxygen plasma power and pressure (50 W and 0.4 mbar, corresponding to an oxygen flow rate of 0.2 Nl/h, respectively).

**2.3. Endothelial Cell Culture in PDMS or UV-PDMS Substrates.** Human umbilical vein endothelial cells (HUVECs) were isolated from freshly obtained human umbilical cords donated under informed consent from mothers and following the method as previously described.<sup>24</sup> All of the procedures were approved by the Ethics Committee for Clinical Research at Galicia (Spain), according to the World Medical Association Declaration of Helsinki. Briefly, HUVECs were cultured on 0.2% (w/v) gelatin (Sigma-Aldrich; Merck Life Science S.L.U., Madrid, Spain) precoated flasks or dishes (Corning, New York, NY, USA) and grown in complete EGM-2 media (endothelial growth medium-2, Lonza, Basel, Switzerland), containing 2% fetal bovine serum (FBS) between other components, in a humidity-saturated atmosphere with 5% CO<sub>2</sub> at 37 °C (MCO-170AC-PE CO<sub>2</sub> incubator, PHCbi). Cells for the experiments were used between the second and seventh passages.

For cell adhesion and cell growth experiments, the 40 mm-glass Petri dishes filled with PDMS or UV-PDMS (with or

without different surface treatments, T1–T3) were sterilized by autoclavation (121 °C, 60 min) and precoated with 0.2% gelatin in phosphate-buffered saline (PBS) during at least 30 min in the cell culture incubator. Six-multiwell polystyrene plates were precoated in the same way and used as the standard surface for cell culture (6-well multiplate, ref. 3516, Costar). For these experiments, confluent HUVEC cultures were detached with 0.25% trypsin (in ethylene-diamino-tetraacetic acid solution; Gibco) and seeded in the Petri dishes or multiwell plates at a concentration of 10,000 cells/cm<sup>2</sup> (LUNA-II cell counter, Logos Biosystems). For the comparison of the effects of different OPT durations, HUVECs were seeded in the same way as described above.

For HUVEC seeding in the Y-shaped channels, these were precoated with fibronectin (5 μg/mL in 0.02% gelatin solution in distilled water) for at least 3 h at 37 °C. After that, HUVECs were seeded in two rounds: one for one side of the channel and another 3 h later in the opposite side of the channel. On each case, at a concentration of 10<sup>6</sup> cells/mL. After the last seeding, the channels were kept in the cell incubator overnight under static conditions of culture. This allowed the establishment of a confluent monolayer of the HUVECs in the inner surface of the channel. The details about the settings on the flow experiments are gathered in Section 2.5.

**2.4. Observation and Staining of HUVECs.** Cell adhesion to the PDMS or UV-PDMS surfaces was evaluated at 3 h after HUVECs seeding. Cells were photographed under phase contrast microscopy with 100× and 200× magnification (model IXS1, Olympus, L'Hospitalet de Llobregat, Spain). Images were processed with CellSens software (Olympus).

Cell growth was measured after 24 h of HUVECs culture in the surfaces under analysis by phase contrast microscopy or fluorescent microscopy. For that, cells were stained with calcein AM (acetoxymethyl ester), a fluorescent cell viability probe. Calcein AM was incubated with HUVEC, prior to imaging, during 5 min at 37 °C (2 μg/mL, final concentration) for cell loading. After this time, the calcein solution was replaced with complete EGM-2 medium, and cells were observed and photographed under a fluorescence microscope (calcein optimal excitation/emission wavelengths: 494/517 nm). Cell growth progression was followed at 48–96 h of culture by phase contrast imaging.

Cell morphology and spreading were analyzed under field emission scanning electron microscopy (FESEM) after 24 h of HUVEC in culture over different materials (PDMS or UV-PDMS) and on UV-PDMS after the different treatments. For that, HUVEC at a concentration of 10,000 cells/cm<sup>2</sup> was seeded in all the surface conditions and after 24 h cells were fixed with 4% paraformaldehyde (PFA) in PBS for 15 min at room temperature. After a PBS wash, samples were dehydrated through a series of increasing ethanol solutions until absolute ethanol was reached, which was dried at room temperature in the flow cabinet. The samples were subsequently studied using a ZEISS FESEM GEMININI-500 microscope (Zeiss; Oberkochen, Germany). Data were acquired at 10 kV.

To observe F-actin filaments, HUVECs were fixed after 24 h of cells' culture with 4% PFA in PBS for 15 min at room temperature. F-actin filaments were stained with fluorescent-conjugated phalloidin (1:1000 dilution in 1% bovine serum albumin in PBS of commercial phalloidin stock solution, Phalloidin CruzFluor 594 Conjugate, ref. sc-363795, Santa Cruz Biotechnology), and nuclei were stained with Hoechst 33342 (a ready-to-use solution of NucBlue Live ReadyProbes



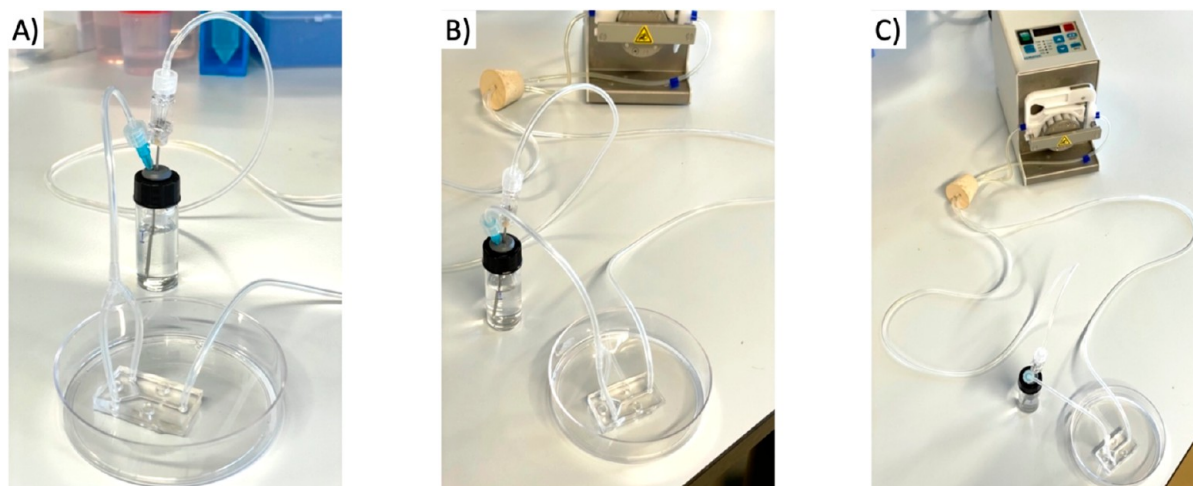


**Figure 1.** Setup of a circuit assembly for flow application on a microfluidic device. (A) Close-up view of the device and its connection to the medium reservoir bottle. (B) View of the circulation through the chip of the fluid coming from the pump and exiting through the medium reservoir. (C) Panoramic view showing the integration of the peristaltic pump, the chip, and the reservoir bottle in the circuit as a whole.

Reagent; Invitrogen). F-actin filaments were observed by red fluorescence (CruzFluor 594 Conjugate: 590/618 nm wavelengths, ex/em) and nuclei by UV excitation and blue emission (460 nm) in a confocal microscope (Leica SP8, Leica microsystems, Wetzlar, Germany). The images were processed with Leica software (LAS X, Leica microsystems, Wetzlar, Germany). The experiments were always performed in triplicate. Image for this set of experiments was analyzed with the “Directionality” analytical tool and the “OrientationJ” plugin of ImageJ (1.53 version) to check the main orientation angle of the filaments.

**2.5. Flow Experiments in UV-PDMS Chips.** For the application of flow on the UV-PDMS channels, a closed circuit was set up by using a peristaltic pump (REGLO digital model, Ismatec, Vancouver, WA, US). Silicone tubes (3 mm external diameter and 1 mm internal diameter) previously sterilized by autoclavation were connected in the inlet and outlets of the Y-shaped UV-PDMS channels. Tubes from the channel’s outlets were collected together in a glass bottle with a rubber septum in the lid and filled with 6 mL of EGM-2 medium. From this reservoir, medium was aspirated by the peristaltic pump with a long needle and reintroduced in the UV-PDMS channels (Figure 1). The circuit was introduced in the cell culture incubator to perform the experiment at 37 °C under the conditions of cell culturing.

Flow experiments were started the morning of the next day, with the seeding of cells in the channels. A stream of growth medium was applied, starting from 0.5 mL/min and increasing progressively in 1 h intervals until reaching the desired final flow rate, where the experiment was maintained for 6–7 h. Experiments were performed at four different flow rates in the range of 1.5 to 6 mL/min (1.5, 2.5, 4, and 6 mL/min). After each setting, the flow was stopped, and cells were fixed with 4% PFA for 15 min. Subsequently, nuclei were stained with Hoechst 33342 (NucBlue Live ReadyProbes Reagent; Invitrogen). Finally, the nuclei of HUVECs at the level of the main branch, the bifurcation, and the two branches of the channel were observed and photographed under a fluorescence microscope.

**2.6. Data Analysis.** The open source image editing software ImageJ<sup>25</sup> was used to assess cell growth. Cell counting and calculation of the total area occupied by cells in the

observed field were performed using the calcein-stained images, following the threshold protocols of the software to differentiate the “occupied” pixels from the “free-of-cells” pixels. Finally, the analytical function of the software was used to obtain the numerical values of the areas and the number of particles analyzed, which were later used in the Excel (Microsoft) software to construct the graphs and perform the statistical analysis using the Student’s *t*-test to compare the differences between treatments and control. In the experiments to test the adhesion of HUVECs to UV-PDMS under different times of OPT, the number of cells in different fields of the culture was counted manually by two independent observers. Unless any comment specifying it, the experiments were made at least by triplicate. Data were expressed as the mean  $\pm$  s.e.m. (standard error of the mean). Significant differences were considered when  $p < 0.05$ .

In the case of HUVECs adhesion to the different UV-PDMS treatments and for cell growth evaluation, a qualitative assessment was made by observing the cell state according to the quantity or intensity of the observed parameter. Three grades were established to represent: (+) a low number of cells with a poor cell arrangement, as assessed by cell spreading, clustering, and surface occupation; (++) a significant number of cells with noticeable cell arrangement, demonstrated by their spreading, clustering, and surface occupation; and (+++) cell confluency or near confluency, exhibiting excellent cellular conformation in terms of cell spreading, clustering, and surface occupation (resembling a “cobblestone” morphology). The confirmation of the grade on this analysis required the agreement of two independent observers. This type of qualitative analysis was also used in the assessment of cell growth with images at 48–56 h post seeding and at 24 h in the UV-PDMS experiments with different OPT times. In the analysis of cell morphology and orientation by phalloidin and Hoechst 33342 staining, the distribution of F-actin filaments and nuclei in the different treatments was considered. Cell anisotropy was calculated for each imaged cell after staining with the Phalloidin CruzFluor 594 Conjugate for F-actin visualization. The degree of anisotropy was calculated by the ratio of the lengths of the long and short axes of each cell. In the experiments with flow application to the UV-PDMS chips, a qualitative and quantitative assessment was used based on the

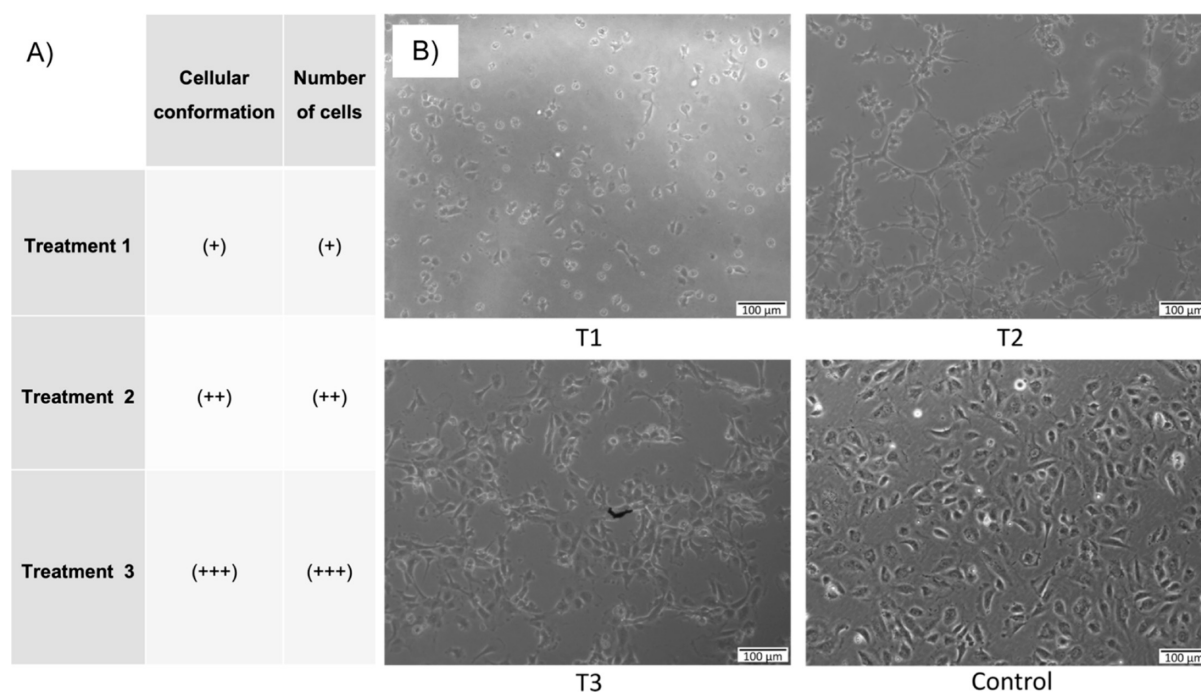


**Figure 2.** Cell adhesion. (A) Assessment of cell status at 3 h post-seeding in the different treatments. Three-grade scale: (+) low level, (++) intermediate level, and (+++) high level, as detailed in the [Methods Section](#). (B) Representative images of the cell state at 3 h post-seeding. T1: normal production without treatment; T2: water boiling; and T3: oxygen plasma treatment. Control: standard polystyrene surface for cell culture.

presence or absence of more than 90% HUVECs occupancy in the observed fields. Images from different locations of the chips (main channel, bifurcation, and daughter arms) were processed with ImageJ (“Analyze Particles” tool) to quantify the number of cells per surface unit.

In order to assess the hydrophobic recovery behavior of the samples, the wettability of untreated and water boiling and OPT treated UV-PDMS samples in terms of water surface contact angle (CA) was measured. The wettability of a solid surface is an important physical property from a practical point of view and depends on the chemical composition and microstructure of the surface. First, CA was measured immediately after the preparation of the samples and then measured after 4 and 7 storage days. Samples were stored in sealed Petri dishes until measurements. The static CA was determined with ImageJ using DropSnake-plugin,<sup>26</sup> which uses active contours (energy minimization) to track the outline of the drop and calculate CA.

### 3. RESULTS

**3.1. Comparison between PDMS and UV-PDMS.** The behavior of the HUVEC culture over surfaces of PDMS or UV-PDMS was first compared. HUVECs were seeded in surfaces made from these materials, and their morphology and viability were checked after 24 and 48 h in comparison with conventional polystyrene culture plates. HUVECs were able to adhere to both PDMS materials and create a viable culture after 48 h ([Figures S1 and S2](#)). Cells seem not to spread and grow at the same velocity as in conventional plastic material. However, the experiment confirmed two issues: (1) both PDMS materials were biocompatible with HUVECs culture, and (2) the optical quality of UV-PDMS for microscopy was really good, surpassing that of PDMS ([Figures S3 and S4](#)).

[Figure S3](#) presents a qualitative examination of the top surface topography acquired using phase contrast microscopy,

under identical acquisition conditions, depicting cells seeded on (A) thermally cured PDMS and (B) UV-cured PDMS. FESEM images of the unseeded top surfaces of (C) thermally cured PDMS and (D) UV-cured PDMS reveal significantly larger numbers of digs in the thermally cured PDMS when compared to UV-PDMS. Remarkably, this distinction in material imperfections is consistently observed, even when imaging deep within the material.

On the other hand, transmission spectra of representative sheets of thermally cured PDMS and UV-cured PDMS were measured with a UV/vis spectrometer (PerkinElmer Lambda 25 UV/vis Spectrophotometer, PerkinElmer Inc., Waltham, Massachusetts). As shown in [Figure S4](#), both PDMS materials are highly transparent from the UVA to the NIR spectral region, with very flat behavior in the visual region. A higher transmittance spectrum on the UV-PDMS substrate in the visible and NIR light domain is attained with an increase of approximately 5% compared to thermally cured PDMS.

Additionally, we studied the combination of different ratios of A and B components to prepare UV-PDMS, to test which proportion showed better biocompatibility. HUVECs were cultured for 24 h in UV-PDMS surfaces prepared from a range of proportions of A and B components of 40–60%. As shown in [Figure S5](#), the best ratio for HUVECs adhesion and growth at 24 h was the mix of 50:50 weight ratio of the two components. This was estimated by counting the number or adhered-living cells after 24 h of culture and/or the number of cells’ clusters formed. As a result, 50:50 was the ratio used in the rest of the experiments with UV-PDMS.

**3.2. Adhesion and Growth of HUVEC on UV-PDMS.** Cell adhesion was assessed 3 h after HUVECs seeding on the different surfaces. In comparison to the control in polystyrene multiwell plates, the UV-PDMS treatment type was evaluated following the 3-grade scale. The results are summarized in [Figure 2](#). OPT (T3) resulted in a high level of cellular

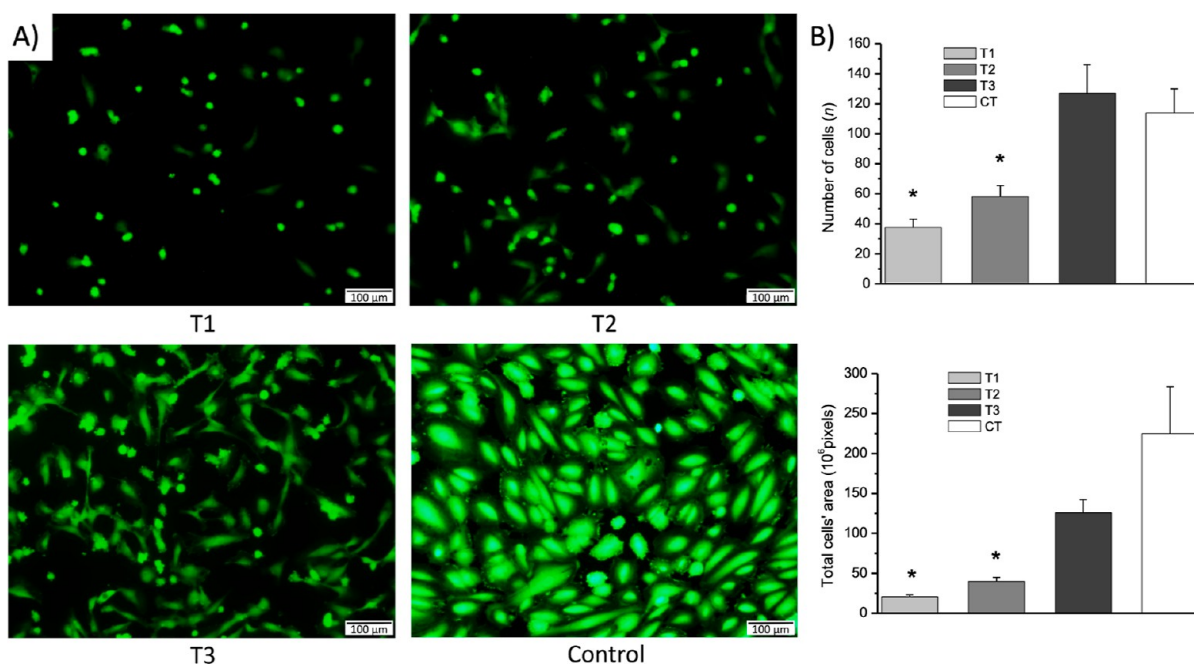


**Figure 3.** Cell growth. (A) Representative images of cell state at 24 h post seeding in UV-PDMS (T1, T2, and T3) or in standard polystyrene surface for cell culture (control). (B) Cell area and number of cells in each condition. \* $p < 0.05$  for the comparison with the control. T1: normal UV-PDMS without treatment, T2: UV-PDMS boiled with water, and T3: UV-PDMS treated with oxygen plasma.

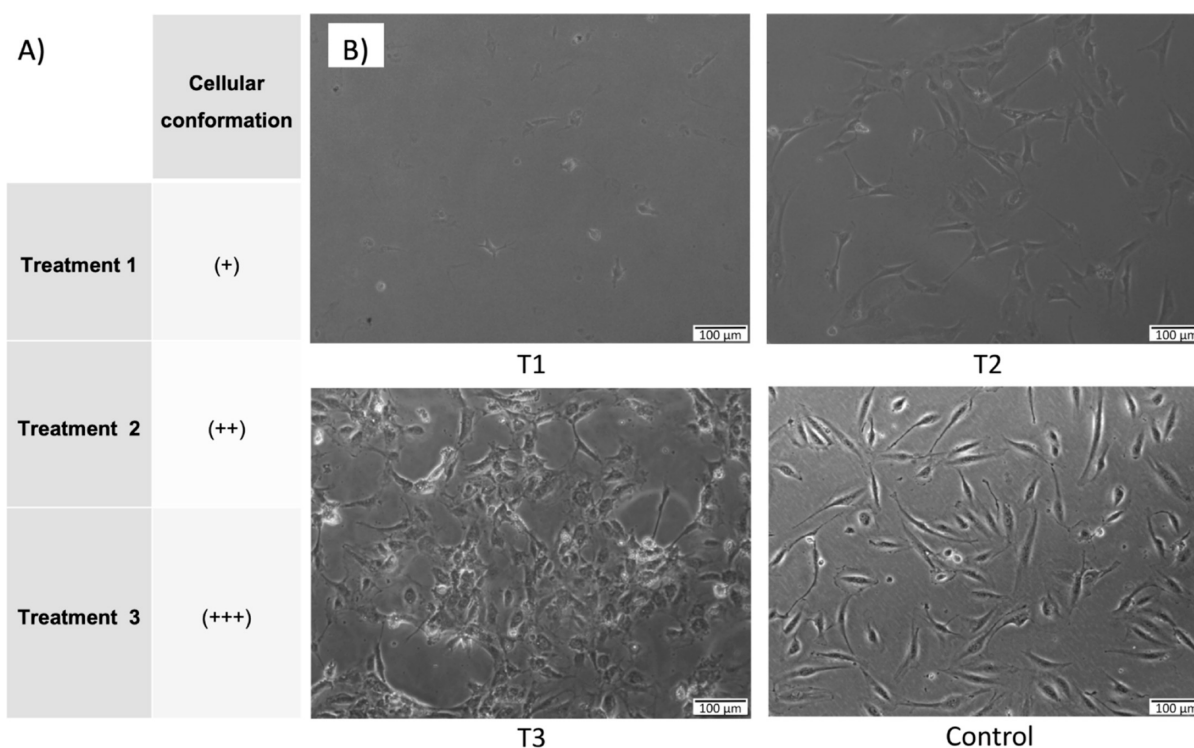


**Figure 4.** Cell growth and maintenance. (A) Assessment of the cell growth trend in T1, T2, and T3. Three-grade scale: (+) low level, (++) intermediate level, and (+++) high level, as detailed in the Methods Section. (B) Representative images of cell growth at 72 h under phase contrast microscopy. T1: standard production without treatment; T2: water boiling; T3: oxygen plasma treatment; and control: polystyrene.

conformation (analyzing cell stretching, cell clustering, and occupation of the culture surface) and a cell number of the same level. Treatment with boiling deionized water (T2) also showed a noticeable cell arrangement in addition to a good number of cells, both with an intermediate level and lower than in the first case. Finally, the common UV-PDMS fabrication

without treatment (T1) showed the lowest cell adhesion capacity with a worse cell arrangement compared to the other two treatments, in addition to a low number of cells.

Cell growth was assessed 24 h post-seeding. The following results were obtained from the images obtained with calcein staining method. Using ImageJ software, the number of cells



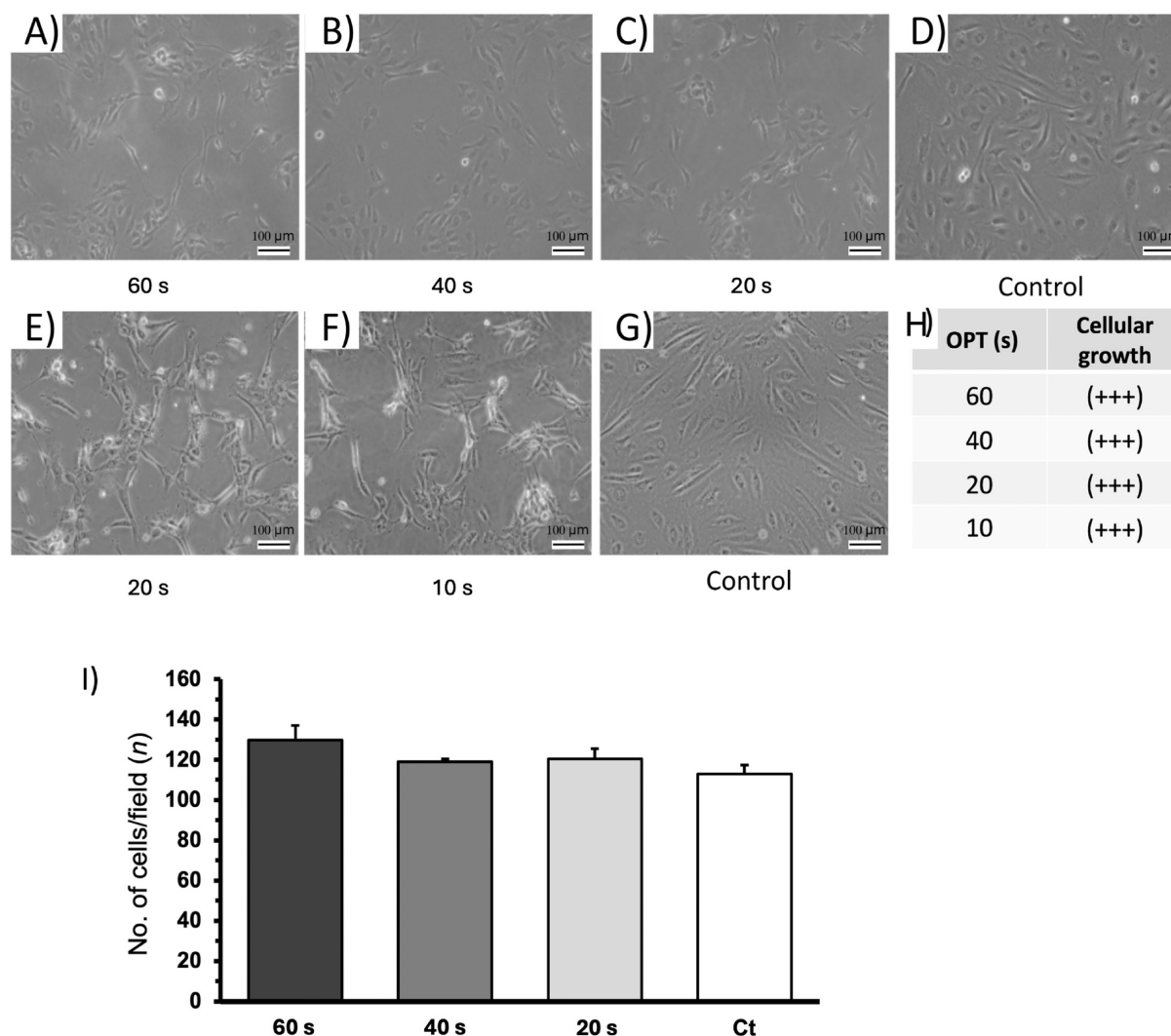


**Figure 5.** Optimization of oxygen plasma treatment (OPT). Representative images of cell growth in the comparative experiments with 60, 40, 20, and 10 s of the OPT (A–C,E–F) and the control in polystyrene (D,G). Scale bar is the same in all cases: 100  $\mu\text{m}$ . Table with assessment of cell growth for the different OPT times (H). Number of cells on each condition after 24 h of culture (I), with columns representing the mean value of cells/area and s.e.m. by the bars.

and the degree of cell occupation on the culture surface were quantified by calculating the total area occupied by the cells in the image field. The results showed two important findings. In the one hand, the number of adhered-living cells after 24 h of culture was similar between the control surface and the UV-PDMS with the OPT (no statistical differences,  $p > 0.05$ ). However, the number of cells was significantly less ( $p < 0.05$ ) in the UV-PDMS treated with boiling water or without any treatment, in comparison to the control. In the other hand, the area of surface occupied by HUVECs in the cultures of T1 and T2 conditions was significantly lower than in control ( $p < 0.05$ ). On the contrary, no statistical differences were found between T3 and control ( $p = 0.108$ ). The results are shown in Figure 3.

Differences in cell morphology and shape were also observed, with the control showing a larger cell size and circularity (isotropy) and the cells fully stretched on the culture substrate and with the cell outline easily differentiated. The UV-PDMS treatments (any of them) showed a different morphology, with a more elongated and less circular morphology (anisotropy); in addition, the cells were much

less agglutinated, and the limits of the cell outlines were more difficult to observe.

The images taken between the second and fourth days of culture (48–96 h after seeding HUVECs) were used to analyze the trend in HUVECs growth in the different treatments. Thus, we see that in T3, the trend toward confluency and cell growth is progressive and high, in the case of T2, this trend is not so pronounced but growth continues, presenting an intermediate level, and in T1, it is much lower, where we barely observe cell clusters in comparison with the other treatments (Figure 4). The general appearance, even in the T3 condition was never exactly the “cobblestone-like appearance”, unless confluency were reached.

Finally, a last analysis was made to assess the possible loss or decrease of the properties acquired on the UV-PDMS plates after exposure to air after the OPT treatment. For this purpose, the previous experiments were carried out with different post-OPT times, observing if the cell culture showed differences between them. Plates with 3, 5, and up to 8 days of exposure were used, and the results showed no appreciable differences in

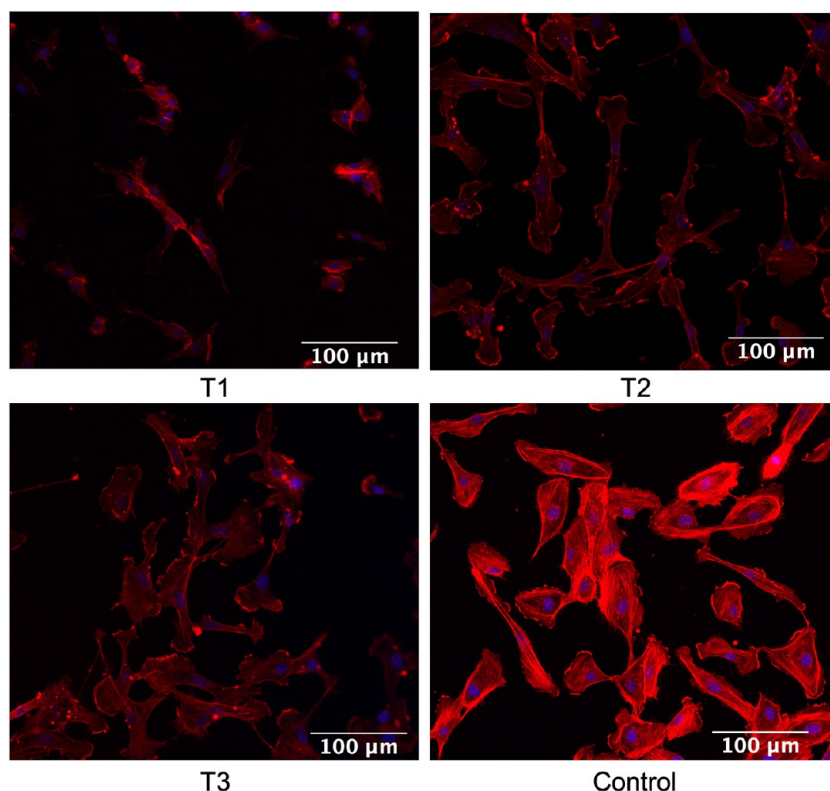


**Figure 6.** Cell morphology adaptation. Representative images of the distribution of F-actin filaments stained with fluorescent-conjugated phalloidin (red) and nuclei, stained with Hoechst 33342 (blue), in the different surfaces. T1: standard production without treatment; T2: water-boiled; T3: oxygen plasma treatment; and control: polystyrene.

cell adhesion or growth for the different times (data not shown).

The time of the OPT needed to obtain the results of enhanced cell adhesion was studied. For that, UV-PDMS surfaces were subjected to different OPT times (from 10 to 60 s). In Figure 5, it can be observed that after 24 h of seeding, HUVECs growth was similar in all the conditions and of good quality and quantity in comparison with polystyrene control surfaces. The number of cells after the same time of culture was quantified for each condition and compared between groups, showing no statistical differences between them (Figure 5, panel I).

Previous works have observed that OPT can be applied on PDMS films as a surface modification method to increase hydrophilicity and roughness modifications that significantly boost cell attachment and proliferation.<sup>27</sup> To assess the hydrophobic recovery behavior of the samples, the wettability of untreated, water boiling, and OPT UV-PDMS samples in terms of water surface CA was measured. Experimental data are shown in Figure S6, where it can be observed that right after the treatments were performed, the CA of untreated UV-PDMS samples declined from about 108 to 64.5° after only 10 s plasma exposure, 45.2° for 20 s, 24.3° for 40 s, and 14.8° for 60 s. As the water CA diminishes, the surface wettability increases consequently. This decline in CA can be attributed to surface oxidation during plasma treatment, transforming the PDMS surface into a SiO<sub>x</sub> surface with hydrophilic properties. However, this higher hydrophilicity is only transient; after a period of storage, the CA increases in all cases, as evidenced in Figure S6. For water boiled samples, the CA reduction is significantly lower than for the OPT-treated samples, with this

value being about 97.7° and which barely varies during the 7 storage days. Interestingly, for all cases, the treated samples did not fully regain the initial hydrophobicity of the untreated UV-PDMS films, suggesting the presence of residual polar groups on the UV-PDMS surface even after 7 days of storage.

**3.3. Cell Morphology and Orientation.** Cell morphology and spreading were first analyzed by FESEM. As shown in Figure S7, no appreciable differences were observed between HUVECs on the different materials (PDMS or UV-PDMS). Apparently, cells can spread their cytoplasm over the surfaces, and no appreciable differences could be observed by this technique. Regarding the treatments of UV-PDMS, water-boiling or OPT did not induce significant changes in the morphology of HUVECs, compared between them, as studied by FESEM.

We observed the arrangement of F-actin and stress filaments in HUVECs cultured on different surfaces after staining with fluorescent-conjugated phalloidin. In our experiments, F-actin filaments were mostly concentrated at the periphery of the cells or surrounding the nuclei, where we perceived a band with a brighter hue in the three conditions of UV-PDMS treatment and the control (Figure 6).

Some stress fibers were also observed at the intracellular level, especially in the control, but this could be due to the better optical quality shown by the standard culture surface in comparison with the UV-PDMS preparations. The main degree of orientation of the F-actin filaments was obtained with ImageJ and expressed in color map coding (Figure S8). Filaments were oriented in all cases in the direction of the long axis of the cell or around the nucleus. It can be seen in some cases that the direction of the fibers is oriented toward cells in



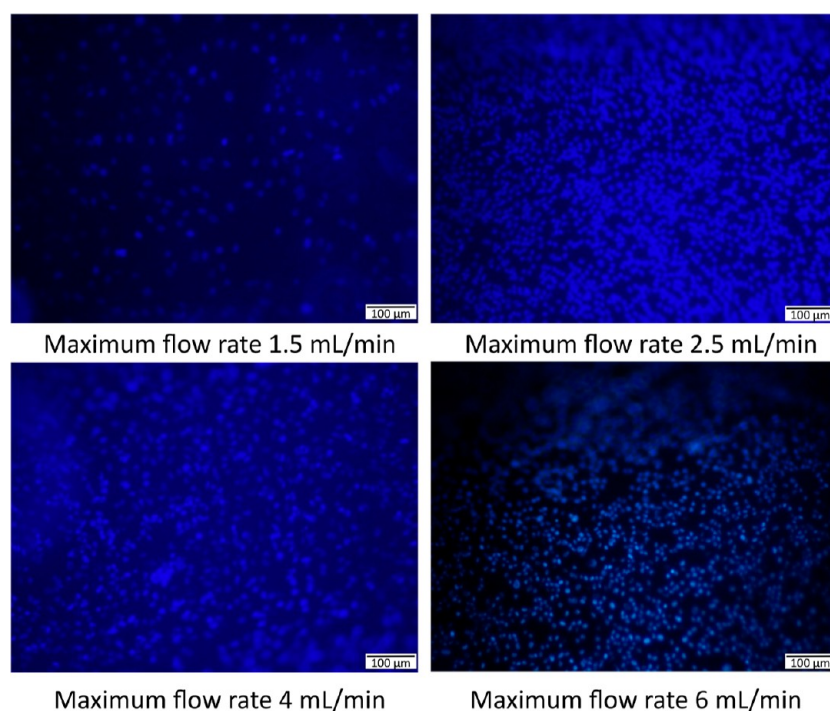


**Figure 7.** Cell culture under flow conditions. HUVECs nuclei stained with Hoechst 33342 in the main branch of the Y-shape channels, observed after exposure to the indicated flow rates for 6–7 h.

close proximity in search of contact with them, but in general, the fibers are spread out randomly. Therefore, there was no predominant orientation. On the other hand, in the cases of T1, T2, and T3 treatments, F-actin remained concentrated in the peripheral band, and stress fibers were not seen in such a marked way. Finally, the nuclei of the cells were examined with Hoechst 33342 to observe their distribution and size, but no appreciable differences between treatments were observed in terms of size or genetic material condensation.

Although a qualitative change in the arrangement of F-actin filaments was not observed between the different UV-PDMS treatments, the analysis of the cytoskeleton anisotropy showed interesting data. As presented in Figure S8, this degree was significantly increased in cell culture over UV-PDMS with OPT in comparison to control surfaces.

Optical images utilizing UV-PDMS microfluidic chips have revealed a significantly better optical quality compared to thermally treated PDMS microfluidic chips. Specifically, the optical clarity and transparency of the UV-PDMS microfluidic chips allowed for higher resolution and more accurate observations of the cells cultured within the channels. Our findings suggest that the use of UV-PDMS microfluidic chips can enhance the sensitivity and accuracy of microscopy experiments and enable researchers to study small-scale phenomena with greater detail.

**3.4. Cell Adhesion on UV-PDMS Chips under Flow Conditions.** Cell adhesion and viability of HUVECs in channels of UV-PDMS were first tested. Channels based on the conditions of fabrication used showed good properties for HUVECs adhesion, and after 7 h of culture in static conditions, cells formed a confluent monolayer in all the locations of the channel (Figure S9). They were also in a good state of viability, as demonstrated by calcein-AM staining (Figure S10).

In the flow experiments, UV-PDMS chips subjected to the OPT were used to seed HUVECs and analyze their behavior

under different flow conditions in a range of 1.5–6 mL/min (1.5, 2.5, 4, and 6 mL/min). After reaching the maximum flow rate, this was maintained in all cases for 6–7 h. Quantification of the HUVECs that still adhered to the channel's walls after exposure to the flow was done by staining the nuclei of the cells with Hoechst 33342.

It was confirmed that from the lowest flow rate of 1.5 mL/min to the maximum flow rate of 6 mL/min applied, cell occupancy after flow exposure was maintained in all the observed portions of the channel (main channel, bifurcation point, and side branches of the channel). Counts of HUVECs nuclei per surface unit were indistinguishable from one condition to another (data not shown). Cell occupation was always >90% of the wall surface (Figure 7).

#### 4. DISCUSSION

The present work has demonstrated the following important points. First, UV-PDMS showed a better optical quality than normal PDMS, with similar biocompatibility. Second, the surface of the UV-PDMS can be subjected to postproduction processes that improve its qualities for cell adhesion and growth. An acceptable protocol for the OPT was found in our experiments. Third, the optimized conditions of the OPT were checked in the surfaces of UV-PDMS channels, where HUVECs were cultured and subjected to different conditions of flow rates, with successful results.

PDMS is the most used material for the fabrication of 3D microfluidic chips and organ-on-a-chip models not only because of its qualities of biocompatibility, nontoxicity, high gas permeability, and optical transparency but also because of its simple and accessible manufacturing techniques. However, in our preliminary experiments, a type of PDMS cured by UV light (UV-PDMS, prepared from KER-4690 A/B), showed easier and faster manufacturing techniques. Importantly, we could also observe improved optical transparency in

comparison with PDMS, maintaining its other properties. It also showed the common hydrophobicity to all PDMS, which makes the adhesion of cells to its surface difficult. However, these results encourage efforts to optimize UV-PDMS surfaces for cell culture, given their better optical quality and advantages in the fabrication process. Optical quality and transparency are critical characteristics in microfluidic chips because they enable researchers to visualize, detect, calibrate, and ensure the compatibility of the chip and its contents. Many microfluidic applications require the use of optical detection methods to analyze the contents of the fluid. For example, fluorescence microscopy is commonly used to detect and quantify biological molecules such as DNA or proteins, both in the cells seeded on the chip and in the liquid flowing in the microfluidic circuit. The optical quality and transparency of the chip directly affect the sensitivity and accuracy of these detection methods.

Two different treatments were applied on UV-PDMS and compared with nontreated UV-PDMS and with conventional polystyrene culture plates regarding the behavior of HUVECs in culture. The treatments involved boiling the UV-PDMS surface with deionized water for 1 h and using an OPT at a pressure of 0.4 mbar for 60 s. After these treatments, two important issues of cell culturing were explored with HUVECs. First, cell adhesion, the initial mandatory step for all adherent cultures, was tested after 3 h of seeding HUVECs in the different surfaces at a cell density enough to initiate a culture but not enough to cover the entire surface. We could observe that the OPT showed better data at this step, in comparison with no-treatment and with treatment with boiling water. Importantly, it showed no significantly different behavior compared with a conventional plastic surface.

Second, after cell adhesion, the next challenge for every cell culture is cell growth: cell division and adhesion to the surface of the daughter cells, forming growing colonies, and spreading over the surface to form a monolayer of cells. For that, the evolution of the cultures was checked after 24 h of cell seeding, time enough to follow the cell's division and the start of cell culture growth. It was possible to observe that cell growth at 24 h post-seeding in the different treatments showed a greater development in the case of OPT compared to the other treatments and was not significantly different from the control in conventional plastic culture. Cells' area and number of cells were quantified to statistically compare the behavior on each treatment. This trend was maintained about the observations made at 46–98 h post-seeding, where we observed again the higher performance of the OPT.

Calcein AM was used to measure the viability of cells since this is a fluorescent probe that needs the cells to be alive to enter and be retained inside them. Therefore, apart from visualization and image analysis, this probe helped to confirm the viability of the HUVEC culture. Another important point is cell morphology, which can be quite characteristic of some cell types. In this sense, endothelial cells present a typical morphology in culture that orientate about their functioning.<sup>28</sup> HUVECs in culture normally spread their cytoplasm and elongate, looking for connections with the surrounding cells. They grow until confluency of the culture, a situation that inhibits their division and induces the adoption of the typical "cobblestone" morphology as stationary culture.

These results encouraged us to look for the best protocol of application of the OPT to improve its advantages. Therefore, different times of application of the OPT on the UV-PDMS

were tested for the HUVEC culture. Regarding this, no differences were observed in terms of cell adhesion and growth in the range of times analyzed, which arouses greater interest in the use of the shorter OPT time. Moreover, prolonged or excessive exposure to oxygen plasma can lead to the oxidation and degradation of the polymer surface, resulting in changes in the material properties and appearance affecting to its optical quality, mechanical strength, stiffness, and elasticity.<sup>29,30</sup> One of the common effects of a longer OPT on PDMS is the yellowing or darkening of the material, affecting its transparency. The obtained results suggest that UV-PDMS treatments with boiling deionized water and OPT may be a possible explanation for the increased hydrophilicity of the polymer surface, which is in agreement with the investigations of Park et al.,<sup>23</sup> Tan et al.,<sup>31</sup> and Bodas and Khan-Malek,<sup>32</sup> as it contributed to the improved adhesion and growth capacity of HUVECs compared to the untreated configuration. Our results also demonstrated higher cell growth and adhesion capability for UV-PDMS plates with OPT compared to the other treatments.

It is important to recapitulate that, to this point, the application of the OPT to the UV-PDMS has improved the biocompatibility of the material, from the point of view of cell adhesion in the first hours of culture, cell growth, and cell spreading during the first 24 h of culture, and in terms of culture progression after 24 h. In all of these parameters, the OPT has allowed a similar performance of the UV-PDMS comparing the standard surfaces for cell culture. However, although quantitatively there were no differences between the OPT and control surfaces in these parameters, the idea that the HUVECs morphology was not the same on both surfaces persisted. Therefore, this point will be analyzed below in terms of cell anisotropy and F-actin filament conformation.

It was observed that, despite what Fritz and Owen<sup>33</sup> and Tan et al.<sup>31</sup> stated about the rapid recovery of hydrophobicity with exposure of the material to air in plasma treatments, in our hands, after several days of UV-PDMS exposure to air, no differences in adhesion and cell growth were observed in the OPT surfaces at the different post-OPT times, retaining the properties acquired with the treatment. This was confirmed by water CA measurements, where, regardless of the duration of the OPT, a consistent trend of wetting behavior is observed across all evaluated UV-PDMS films. Although they regain hydrophobicity after storage, it can be seen from the results that the OPT modification shows reasonably good hydrophilic stability in the range of a week with a CA below 80°, which is consistent with our experimental results where enhanced cell adhesion and growth with the OPT were found and maintained during the duration of the biological experiments.

As for the UV-PDMS tests with different OPT times, very good results were observed in terms of the level of growth for all of them. Therefore, it was determined that there were no appreciable differences in terms of cell growth at 24 h post-seeding with the different treatment times, which leads us to think about the usefulness of using the one with the shortest exposure time to the OPT. It was not possible to appreciate the possible damage due to overtreatment and therefore the differences in growth and adhesion in relation to the study carried out by Jofre-Reche,<sup>34</sup> which suggests that the increase in the hydrophilicity of PDMS is proportional to the exposure time to OPT and a decrease in hydrophilicity is only observed in cases of overtreatment that occur with the creation of weak layers of silicon dioxide on the surface of PDMS, which

decrease cell adhesion. The work of Amerian et al.<sup>27</sup> discusses an ideal plasma exposure time interval that allows the best conditions for cell adhesion and proliferation to be acquired, and this does not coincide with the longest exposure time to OPT, which is consistent with the previous experiment where the creation of weak layers was discussed.

In relation to the distribution of F-actin filaments, it was found that they did not follow an established order in static cultures, with a majority accumulation in the cell periphery and showed little presence of stress fibers. This could be normal since there was no factor stressing the cells to orientate in a particular direction. However, this could also be due to the difficulty of seeing the UV-PDMS surfaces under high microscopic magnification. The culture dishes with this material had several millimeters of thickness, which made it impossible to focus the cells with objectives of low working distance, such as those mounted in the biomedical confocal microscopes. A higher magnification was obtained in the plastic cultures, where stress fibers, oriented mainly in the longitudinal axis of the cells, were observed.

F-actin filaments form elongated bundles formed by the organization of F-actin when the cell is subjected to a stimulus, which contributes to functions such as cell morphogenesis, adhesion, and migration. Phalloidin is a natural peptide that binds to F-actin with high specificity, interacting with polymeric actin and not oligomeric or monomeric forms. The conjugation of phalloidin to a fluorescent probe allowed visualization of these filaments. The stress fibers presented a random arrangement, with a majority accumulation of F-actin in the periphery of the cell forming a kind of band, which is in agreement with the previous work of Inglebert et al.<sup>35</sup> and Tovar-Lopez et al.<sup>36</sup> No differences were observed between the different treatments in terms of the F-actin arrangement. The studies by Inglebert et al.<sup>35</sup> also assessed that these fibers are organized differently depending on the stimuli, leading to their formation and permanence under high stress, e.g., under high flow, and their disorganization under low stress, such as low flow or cells under static conditions. Inglebert et al.,<sup>35</sup> Tovar-Lopez et al.,<sup>36</sup> and DeStefano et al.<sup>37</sup> also observed the variations caused in cells when subjected to turbulent flow, laminar flow, or static conditions. Under laminar flow, the stress fibers were oriented in the direction of the flow, and in turbulent flow, these fibers were oriented perpendicularly to the flow. In the work of Tovar-Lopez et al.,<sup>36</sup> it was observed that the nuclei also vary in shape, being more rounded and smaller in area when the cells are under turbulent flow compared to laminar flow and static conditions. This is attributed to changes in gene expression under different flow dynamics and changes in intracellular signaling. In our experiments, under static conditions, no significant differences in nuclei or cell size were observed between the different treatments.

Taken into account that in UV-PDMS without treatment and in the case of treatment with boiling water, there were no changes with regard to the anisotropy shown by control cultures, this could mean at least two things. First, after the OPT, the surface could be modified and stimulate the migration of HUVECs, promoting a change in their anisotropy degree. Or second, the surface facilitates the anchoring of HUVECs, which facilitates the elongation of the cells, allowing the increase of their degree of anisotropy. These changes could be promoted by the increase of hydrophilicity induced by OPT, as suggested by others.<sup>31,32</sup> In any case, a significant change in cell

morphology could be quantified with this technique, which could be related to an enhanced function of migration or cell adaptation to the surface of culture in the UV-PDMS treated with oxygen plasma.

However, individual cell analysis by FESEM did not show any difference between the cells spreading on different surfaces. This is probably due to the features of the technique. SEM allows for good magnification of cells for individual analysis, but without any staining of the subcellular components, and the global perspective of the culture is difficult to establish. Therefore, some bias could be introduced, as cells with good performance are easier to locate by SEM than poorly adhered cells. In other words, this technique could confirm that it was possible to observe appropriate adhesion of some HUVECs in all the surfaces tested, but global comparison of surfaces' performance was not possible. Therefore, other aspects of the culture such as global cell growth, degree of anisotropy, cell clustering, and progression to cell confluency, needed to be analyzed by other techniques.

The direct application of flow to the cells for a given time allows us to test their ability to adhere to the channel's walls and their resistance to a constant flow and wall shear stress. To test the possible application of UV-PDMS in microfluidic chips, channels with a Y-shape were fabricated with UV-PDMS. The shape of the channels was intended to incorporate different conditions into the flow that mimic the passage of fluids through biological ducts. In this case, a Y-shaped bifurcation with an angle of 90° was designed for the chip. First, it was possible to check that the gas permeability of the UV-PDMS channel was enough to maintain alive a confluent monolayer of HUVECs seeding the inner walls of the channels under static culture conditions. With respect to the experiments with flow application on the chips, the cell adhesion capacity could be studied. It was possible to study the capacity of HUVECs to withstand the mechanical stress caused by the flow of culture medium up to 6 mL/min, preserving cell confluency in all portions of the channels for the different flow rates analyzed. In the different tests, HUVECs remained at more than 90% of surface coverage inside the channel at all flow rate values used and in all of the locations of the Y-shape channel. The structure and dimensions of our channels allowed us to test a wall shear stress up to 1 dyn/cm<sup>2</sup> using culture medium as the fluid. This value is far from the wall shear stress induced by blood flow, classically considered in arteries in the range of 10–20 dyn/cm<sup>2</sup>; however, it would be in the range of the values in veins (10-fold lesser than in arteries<sup>38</sup>). Importantly, the typical conditions used in experimental *in vitro* systems of vessel-on-a-chip are normally below 1 dyn/cm<sup>2,39</sup> which means that we have demonstrated the viability of our models for fluidic experiments in the laboratories worldwide.

## 5. FUTURE RESEARCH

Future studies could measure the rate at which cells would no longer withstand the mechanical stress of flow with new experiments under flow rates higher than 6 mL/min until a cell occupancy of the channel of less than 90% is observed or analyze the orientation of the F-actin filaments in the channels after flow application.

It is important to state that the OPT of UV-PDMS seemed to qualify this material for the biocompatible culture of HUVECs. Also, this will enable deeper analysis of cell functionality in this material, which could cover a wide range



of aspects, from the conformation of the endothelial barrier to cell migration or wound healing, going through a detailed analysis of the production of the endothelial factors, as mediators of their multiple vascular functions.

## 6. CONCLUSIONS

The findings of our investigation provide compelling evidence regarding the biocompatibility of UV-PDMS for HUVECs culture, mirroring observations made with the widely utilized thermally cured PDMS. Additionally, UV-PDMS demonstrated notable advantages over traditional PDMS, including superior optical clarity and enhanced handling and processing characteristics. This was facilitated by markedly shorter curing times and a simplified process enabled by UV light utilization. Furthermore, the surface properties of UV-PDMS could be readily adjusted through the OPT to enhance HUVECs adhesion and growth, rendering it an excellent candidate for constructing 3D scaffolds for cell culture. Flow experiments revealed that OPT-treated UV-PDMS surfaces effectively supported HUVECs without detachment under flow conditions, highlighting its suitability for microfluidic chip applications. In summary, these findings highlight the potential of UV-PDMS in the development of microfluidic chips for cell-based assays and other biological applications.

## ■ ASSOCIATED CONTENT

### SI Supporting Information

The Supporting Information is available free of charge at <https://pubs.acs.org/doi/10.1021/acsomega.4c01148>.

HUVECs seeding, optical transmission spectra, contact angle measurements, analysis of F-actin filaments orientation, and HUVECs viability in UV-PDMS microfluidic channels (PDF)

## ■ AUTHOR INFORMATION

### Corresponding Author

Ana I. Gómez-Varela – *Photonics4Life Research Group, Departamento de Física Aplicada, Faculdade de Física and Faculdade de Óptica e Optometria, Instituto de Materiais (iMATUS), Universidade de Santiago de Compostela, Santiago de Compostela E15782, Spain; [orcid.org/0000-0001-8191-0257](https://orcid.org/0000-0001-8191-0257); Email: [anaisabel.gomez@usc.es](mailto:anaisabel.gomez@usc.es)*

### Authors

Antonio Viña – *Departamento de Farmacología, Farmacia y Tecnología Farmacéutica, Universidade de Santiago de Compostela, Santiago de Compostela 15782 A Coruña, Spain*

Carmen Bao-Varela – *Photonics4Life Research Group, Departamento de Física Aplicada, Faculdade de Física and Faculdade de Óptica e Optometria, Instituto de Materiais (iMATUS), Universidade de Santiago de Compostela, Santiago de Compostela E15782, Spain*

María Teresa Flores-Arias – *Photonics4Life Research Group, Departamento de Física Aplicada, Faculdade de Física and Faculdade de Óptica e Optometria, Instituto de Materiais (iMATUS), Universidade de Santiago de Compostela, Santiago de Compostela E15782, Spain*

Bastián Carnero – *Photonics4Life Research Group, Departamento de Física Aplicada, Faculdade de Física and Faculdade de Óptica e Optometria, Instituto de Materiais (iMATUS), Universidade de Santiago de Compostela,*

*Santiago de Compostela E15782, Spain; BFlow S.L., Edificio Emprendia, Santiago de Compostela 15782, Spain*

Mercedes González-Peteiro – *Departamento de Enfermería, Santiago de Compostela, A Coruña 15782, Spain*

José Ramón González-Juanatey – *Instituto de Investigación Sanitaria de Santiago de Compostela (IDIS), Complejo Hospitalario Universitario de Santiago de Compostela (CHUS), Santiago de Compostela, A Coruña 15706, Spain; Departamento de Medicina, Universidad de Santiago de Compostela, Santiago de Compostela 15706 A Coruña, Spain; Servicio de Cardiología y Unidad de Hemodinámica, Complejo Hospitalario Universitario de Santiago de Compostela (CHUS), SERGAS, Santiago de Compostela 15706 A Coruña, Spain*

Ezequiel Álvarez – *Departamento de Farmacología, Farmacia y Tecnología Farmacéutica, Universidade de Santiago de Compostela, Santiago de Compostela 15782 A Coruña, Spain; Departamento de Medicina, Universidad de Santiago de Compostela, Santiago de Compostela 15706 A Coruña, Spain; Servicio de Cardiología y Unidad de Hemodinámica, Complejo Hospitalario Universitario de Santiago de Compostela (CHUS), SERGAS, Santiago de Compostela 15706 A Coruña, Spain; CIBERCV, 28029 Madrid, Spain*

Complete contact information is available at:

<https://pubs.acs.org/10.1021/acsomega.4c01148>

### Author Contributions

A.I.G.-V. and A.V. contributed equally to this work. A.I.G.-V., A.V., and E.A. contributed to the conception and design of the study and wrote the first draft of the manuscript. A.I.G.-V., C.B.-V., A.V., M.G.-P., and E.A. performed the experiments. C.B.-V., M.T.F.-A., and J.R.G.-J. participated in the methodology design, gave scientific advice, discussed the results, and got financial support. The final manuscript was reviewed and approved by all authors. All authors listed have made a substantial, direct, and intellectual contribution to the work and approved it for publication.

### Notes

The authors declare no competing financial interest.

## ■ ACKNOWLEDGMENTS

This work was partially supported by “La Caixa” Banking Foundation CaixaImpulse Validate 2021 Call (CI20-00200), Xunta de Galicia (ED431B 2023/07), and the grant PID2022-138322OB-I00 funded by MCIN/AEI/10.13039/501100011033 and by “ERDF A way of making Europe”. A.I.G.-V. also acknowledges the grant RYC2022-035710-I funded by MCIN/AEI/10.13039/501100011033 and by ESF Investing in your future.

## ■ REFERENCES

- (1) Gharib, G.; Bütün, İ.; Munganlı, Z.; Kozalak, G.; Namlı, İ.; Sarraf, S. S.; Ahmadi, V. E.; Toyran, E.; van Wijnen, A. J.; Koşar, A. Biomedical Applications of Microfluidic Devices: A Review. *Biosensors* **2022**, *12* (11), 1023.
- (2) Zommiti, M.; Connil, N.; Tahrioui, A.; Groboillot, A.; Barbey, C.; Konto-Ghiorgi, Y.; Lesouhaitier, O.; Chevalier, S.; Feuilloley, M. G. J. Organs-on-Chips Platforms Are Everywhere: A Zoom on Biomedical Investigation. *Bioengineering* **2022**, *9* (11), 646.
- (3) Aymerich, M.; Gómez-Varela, A.; Alvarez, E.; Flores-Arias, M. T. Study of Different Sol-Gel Coatings to Enhance the Lifetime of PDMS Devices: Evaluation of Their Biocompatibility. *Materials* **2016**, *9* (9), 728.

- (4) Guttenplan, A. P. M.; Tahmasebi Birgani, Z.; Giselbrecht, S.; Truckenmüller, R. K.; Habibović, P. Chips for Biomaterials and Biomaterials for Chips: Recent Advances at the Interface between Microfabrication and Biomaterials Research. *Adv. Healthcare Mater.* **2021**, *10* (14), 2100371.
- (5) McDonald, J. C.; Whitesides, G. M. Poly(Dimethylsiloxane) as a Material for Fabricating Microfluidic Devices. *Acc. Chem. Res.* **2002**, *35* (7), 491–499.
- (6) Roppolo, I.; Chiappone, A.; Angelini, A.; Stassi, S.; Frascella, F.; Pirri, C. F.; Ricciardi, C.; Descrovi, E. 3D Printable Light-Responsive Polymers. *Mater. Horiz.* **2017**, *4* (3), 396–401.
- (7) Layani, M.; Wang, X.; Magdassi, S. Novel Materials for 3D Printing by Photopolymerization. *Adv. Mater.* **2018**, *30* (41), 1706344.
- (8) Chidambaram, N.; Kirchner, R.; Altana, M.; Schiff, H. High Fidelity 3D Thermal Nanoimprint with UV Curable Polydimethyl Siloxane Stamps. *J. Vac. Sci. Technol., B: Nanotechnol. Microelectron.: Mater., Process., Meas., Phenom.* **2016**, *34* (6), 06K401.
- (9) Kim, J.; An, H.; Seo, Y.; Jung, Y.; Lee, J. S.; Choi, N.; Bong, K. W. Flow Lithography in Ultraviolet-Curable Polydimethylsiloxane Microfluidic Chips. *Biomicrofluidics* **2017**, *11* (2), 024120.
- (10) Zhang, T.; Jiang, B.; Huang, Y. UV-Curable Photosensitive Silicone Resins Based on a Novel Polymerizable Photoinitiator and GO-Modified TiO<sub>2</sub> Nanoparticles. *Composites, Part B* **2018**, *140*, 214–222.
- (11) Jiang, B.; Shi, X.; Zhang, T.; Huang, Y. Recent Advances in UV/Thermal Curing Silicone Polymers. *Chem. Eng. J.* **2022**, *435*, 134843.
- (12) Akther, F.; Yakob, S. B.; Nguyen, N.-T.; Ta, H. T. Surface Modification Techniques for Endothelial Cell Seeding in PDMS Microfluidic Devices. *Biosensors* **2020**, *10* (11), 182.
- (13) Jastrzebska, E.; Zuchowska, A.; Flis, S.; Sokolowska, P.; Bulka, M.; Dybko, A.; Brzozka, Z. Biological Characterization of the Modified Poly(Dimethylsiloxane) Surfaces Based on Cell Attachment and Toxicity Assays. *Biomicrofluidics* **2018**, *12* (4), 044105.
- (14) Wu, C.-C.; Yuan, C.-Y.; Ding, S.-J. Effect of Polydimethylsiloxane Surfaces Silanized with Different Nitrogen-Containing Groups on the Adhesion Progress of Epithelial Cells. *Surf. Coat. Technol.* **2011**, *205* (10), 3182–3189.
- (15) Juárez-Moreno, J.; Ávila-Ortega, A.; Oliva, A. I.; Avilés, F.; Cauich-Rodríguez, J. Effect of Wettability and Surface Roughness on the Adhesion Properties of Collagen on PDMS Films Treated by Capacitively Coupled Oxygen Plasma. *Appl. Surf. Sci.* **2015**, *349*, 763–773.
- (16) Berdichevsky, Y.; Khandurina, J.; Guttman, A.; Lo, Y.-H. UV/Ozone Modification of Poly(Dimethylsiloxane) Microfluidic Channels. *Sens. Actuators, B* **2004**, *97* (2–3), 402–408.
- (17) Yang, M. T.; Fu, J.; Wang, Y.-K.; Desai, R. A.; Chen, C. S. Assaying Stem Cell Mechanobiology on Microfabricated Elastomeric Substrates with Geometrically Modulated Rigidity. *Nat. Protoc.* **2011**, *6* (2), 187–213.
- (18) Özçam, A. E.; Efimenko, K.; Genzer, J. Effect of Ultraviolet/Ozone Treatment on the Surface and Bulk Properties of Poly(Dimethyl Siloxane) and Poly(Vinylmethyl Siloxane) Networks. *Polymer* **2014**, *55* (14), 3107–3119.
- (19) Kuddannaya, S.; Chuah, Y. J.; Lee, M. H. A.; Menon, N. V.; Kang, Y.; Zhang, Y. Surface Chemical Modification of Poly(Dimethylsiloxane) for the Enhanced Adhesion and Proliferation of Mesenchymal Stem Cells. *ACS Appl. Mater. Interfaces* **2013**, *5* (19), 9777–9784.
- (20) Chumbimuni-Torres, K. Y.; Coronado, R. E.; Mfuh, A. M.; Castro-Guerrero, C.; Silva, M. F.; Negrete, G. R.; Bizios, R.; Garcia, C. D. Adsorption of Proteins to Thin-Films of PDMS and Its Effect on the Adhesion of Human Endothelial Cells. *RSC Adv.* **2011**, *1* (4), 706.
- (21) Alshehri, A.; Al-Rekabi, Z.; Hickey, R.; Pelling, A. E.; Bhardwaj, V. R. Controlled Cell Adhesion on Microstructured Polydimethylsiloxane (PDMS) Surface Using Femtosecond Laser. In *CLEO: 2014*; OSA: Washington, D.C., 2014; p SF2J.4.
- (22) Alshehri, A. M. Femtosecond-Laser-Assisted Spatial Cell Adhesion to Microstructured Surface Geometry. *AIP Adv.* **2021**, *11* (8), 085017.
- (23) Park, J. Y.; Ahn, D.; Choi, Y. Y.; Hwang, C. M.; Takayama, S.; Lee, S. H.; Lee, S.-H. Surface Chemistry Modification of PDMS Elastomers with Boiling Water Improves Cellular Adhesion. *Sens. Actuators, B* **2012**, *173*, 765–771.
- (24) Paradelo-Dobarro, B.; Rodiño-Janeiro, B. K.; Alonso, J.; Raposeiras-Roubin, S.; González-Peteiro, M.; González-Juanatey, J. R.; Álvarez, E. Key Structural and Functional Differences between Early and Advanced Glycation Products. *J. Mol. Endocrinol.* **2016**, *56* (1), 23–37.
- (25) Abràmoff, M. D.; Magalhães, P. J.; Ram, S. J. Image Processing with ImageJ. *Biophot. Int.* **2004**, *11* (7), 36–42.
- (26) Stalder, A. F.; Kulik, G.; Sage, D.; Barbieri, L.; Hoffmann, P. A Snake-Based Approach to Accurate Determination of Both Contact Points and Contact Angles. *Biophot. Int.* **2006**, *286* (1–3), 92–103.
- (27) Amerian, M.; Amerian, M.; Sameti, M.; Seyedjafari, E. Improvement of PDMS Surface Biocompatibility Is Limited by the Duration of Oxygen Plasma Treatment. *J. Biomed. Mater. Res., Part A* **2019**, *107* (12), 2806–2813.
- (28) Liang, J.; Gu, S.; Mao, X.; Tan, Y.; Wang, H.; Li, S.; Zhou, Y. Endothelial Cell Morphology Regulates Inflammatory Cells Through MicroRNA Transferred by Extracellular Vesicles. *Front. Bioeng. Biotechnol.* **2020**, *8*, 369.
- (29) Hemmilä, S.; Cauich-Rodríguez, J. V.; Kreutzer, J.; Kallio, P. Rapid, Simple, and Cost-Effective Treatments to Achieve Long-Term Hydrophilic PDMS Surfaces. *Appl. Surf. Sci.* **2012**, *258* (24), 9864–9875.
- (30) Kim, P.; Hu, Y.; Alvarenga, J.; Kolle, M.; Suo, Z.; Aizenberg, J. Rational Design of Mechano-Responsive Optical Materials by Fine Tuning the Evolution of Strain-Dependent Wrinkling Patterns. *Adv. Opt. Mater.* **2013**, *1* (5), 381–388.
- (31) Tan, S. H.; Nguyen, N.-T.; Chua, Y. C.; Kang, T. G. Oxygen Plasma Treatment for Reducing Hydrophobicity of a Sealed Polydimethylsiloxane Microchannel. *Biomicrofluidics* **2010**, *4* (3), 032204.
- (32) Bodas, D.; Khan-Malek, C. Formation of More Stable Hydrophilic Surfaces of PDMS by Plasma and Chemical Treatments. *Microelectron. Eng.* **2006**, *83* (4–9), 1277–1279.
- (33) Fritz, J. L.; Owen, M. J. Hydrophobic Recovery of Plasma-Treated Polydimethylsiloxane. *J. Adhes.* **1995**, *54* (1–4), 33–45.
- (34) Jofre-Reche, J. A. *Optimization of the Surface Properties of Polydimethylsiloxane by Plasma Treatment for Adhesion Improvement and Durability to Acrylic Adhesive for Medical Applications*; Universitat d'Alacant-Universidad de Alicante, 2014.
- (35) Inglebert, M.; Locatelli, L.; Tsvirkun, D.; Sinha, P.; Maier, J. A.; Misbah, C.; Bureau, L. The Effect of Shear Stress Reduction on Endothelial Cells: A Microfluidic Study of the Actin Cytoskeleton. *Biomicrofluidics* **2020**, *14* (2), 024115.
- (36) Tovar-Lopez, F.; Thurgood, P.; Gilliam, C.; Nguyen, N.; Pirogova, E.; Khoshmanesh, K.; Baratchi, S. A Microfluidic System for Studying the Effects of Disturbed Flow on Endothelial Cells. *Front. Bioeng. Biotechnol.* **2019**, *7*, 81.
- (37) DeStefano, J. G.; Williams, A.; Wnorowski, A.; Yimam, N.; Searson, P. C.; Wong, A. D. Real-Time Quantification of Endothelial Response to Shear Stress and Vascular Modulators. *Integr. Biol.* **2017**, *9* (4), 362–374.
- (38) Roux, E.; Bougaran, P.; Dufourcq, P.; Couffignal, T. Fluid Shear Stress Sensing by the Endothelial Layer. *Front. Physiol.* **2020**, *11*, 861.
- (39) Wang, L.; Chen, Z.; Xu, Z.; Yang, Y.; Wang, Y.; Zhu, J.; Guo, X.; Tang, D.; Gu, Z. A New Approach of Using Organ-on-a-Chip and Fluid-Structure Interaction Modeling to Investigate Biomechanical Characteristics in Tissue-Engineered Blood Vessels. *Front. Physiol.* **2023**, *14*, 1210826.